CHAPTER 33

Wave Spectrum of Breaking Wave

Toru Sawaragi
Professor of Civil Engineering
Osaka University, Suita,Osaka,Japan
and
Koichiro Iwata
Assistant Professor of Civil Engineering
Osaka University,Suita,Osaka,Japan

ABSTRACT

By wave breaking, an incident monocromatic wave is transformed to a wave composed of its harmonic frequency waves inside a surf zone.

Based on a dimensional consideration, the "-1 power law ", the "-2 power law ", the "-2/3 power law " and the "-1/2 power law " on the wave height spectrum ,H(f), are derived as sorts of equilibrium spectra.

These spectra except"-1/2 power law" are shown to agree with experimental data.

1. INTRODUCTION

The authors[1] already revealed that 25% - 40% of total wave energy was dissipated due to a bottom shear friction and a horizontal roller formed by a plunging breaker in a surf zone.

Therefore, the turbulence with air entrainment will be thought to play an important role in the wave energy dissipation. It is necessary to measure an accurate time-history of water particle velocity in order to clarify the characteristics of turbulence, but, it will be impossible by lack of precise measuring instruments.

Since a wave profile is thought to be an expression of turbulence after breaking, it will be expected that some features of turbulence can be deduced by analysing wave surface profiles.

Inside the surf zone, as the authors already clarified,[1] an incident monocromatic wave is transformed to a complicated breaking wave composed of higher frequency component waves due to non-linearity of breaking phenomenon, and dissipates its excess energy which can not be kept for wave motion. Therefore, the wave will be considered to reach some critical state for maintaining the wave motion. In this critical state, there will exist some sorts of critical conditions for wave height distributions of component waves. With this situation,dimensional consideration is an efficient tool for deriving wave height spectral characteristics.

2. DIMENSIONAL ANALYSIS

The physical quantities to be considered in the dimensional analysis of

wave height spectrum,H(f) are gravitational acceleration g, wave frequency f, still water depth h,density of water with air entrainment ρ^*, molecular viscosity of water with air entrainment μ^*, and surface tension K as shown in Eq.(1),

$$H(f) = f\ (\ g\ ,\ f\ ,\ h\ ,\ \rho^*,\ \mu^*,\ K\ )\ . \qquad \text{----------(1)}$$

As the significance of these parameters changes according to four kinds of frequency range such as one of shallow water waves, deep water waves, capillary ripple waves and the frequency range in which viscosity is predominant, important physical parameters must be selected to fit the physical situation.

Firstly, attension is paid to the wave frequency range associated with shallow gravity waves which satisfies the relation of $f<f_1$, in which f_1 is given by Eq.(2) deduced from Eq.(3),

$$f_1 = \sqrt{g\ /\ 4\pi h}\ , \qquad \text{----------(2)}$$

$$h/Lo = 0.50\ , \qquad \text{----------(3)}$$

where, Lo is a wave length of deep water wave. In this case, the influence of surface tension K is unimportant. Furthermore, the direct effect of ρ^* and μ^* is manifest in wave damping, and under the condition with which we are concerned, these two factors may be the second order terms and may be included in the non-dimensional coefficient of wave height spectrum. Therefore, in this region, three quantities such as g, f, and h are predominant physical factors, and wave height spectrum H(f) has a dimension[L], so that the following wave height spectrum is considered:

$$H(f) = f\ (\ g,\ f,\ h,\ \underbrace{\rho^*\ ,\ \mu^*}_{\text{second order}}\ )\ ,$$

$$= G_1\left(\sqrt{gh^3}\ /(\mu^*\ /\rho^*)\right)\cdot\ g^{1/2}\cdot\ h^{1/2}\cdot\ f^{-1}\ ,$$

$$\propto g^{1/2}.h^{1/2}.\ f^{-1}\ , \qquad \text{----------(4)}$$

$$\text{for } f<f_1\ (=\sqrt{g/4\pi h})\ .$$

Next, consider the frequency range of $f_1<f<f_c$, where f_c is given by Eq. (5)[2],

$$f_c = \frac{1}{2\pi}\sqrt{\frac{\rho^* g}{K}}\ . \qquad \text{----------(5)}$$

This frequency range corresponds to those of deep gravity waves and surface tension K is unimportant as the previous case. ρ^* and μ^* are treated by combining with h as the second order terms, then the predominant physical factors are g and f. Therefore, the following wave height spectrum is considered:

$$H(f) = f(g, f, \{\mu^*, \rho^*, h\}),$$
$$= G_2(\sqrt{gh^3}/(\mu^*/\rho^*))\, g\cdot f^{-2}$$
$$\propto g\cdot f^{-2}, \quad \text{for } f_1 < f < f_c \quad . \qquad (6)$$

In deep gravity waves, Michell[3] gave the critical wave steepness as a breaking condition as shown in Eq.(7):

$$(H/L)_b = 0.142 \quad . \qquad (7)$$

By using the relation of $L=(g/2\pi)f^{-2}$, the critical wave height H(f) is given as follow:

$$H(f) = 0.0226 g f^{-2} \quad . \qquad (8)$$

Comparing Eq.(6) with Eq.(8), the physical meaning of the dimensional analysis is clear and it may be pointed out that the wave height distribution is limited so as to satisfy a sort of critical wave steepness.

As mentioned above, for a frequency range in which a restoring force is gravitational acceleration, the wave height spectrum H(f) consists of Eq.(4) and Eq.(6). By combining Eq.(4) and Eq.(6), the following expression may be possible:

$$H(f) = G^*(\sqrt{gh^3}/(\mu^*/\rho^*))\, g f^{-2}(\tanh(2\pi h f^2/g))^{1/2},$$
$$\propto g f^{-2}(\tanh(2\pi h f^2/g))^{1/2}, \quad \text{for } f < f_c \quad . \qquad (9)$$

For a frequency range of $f<f_1$, the relation of $(\tanh(2\pi hf^2/g))^{1/2} \cong (2\pi hf^2/g)^{1/2}$ is established, and then, $H(f) \propto \sqrt{gh}f^{-1}$ is easily deduced.

Secondly, aiming at the wave frequency ($f_c<f<f_k$) associated with capillary ripples, the influence of gravitational acceleration is ignored, where, f_c is given by Eq.(5), and f_k is the highest frequency for which the surface tension is predominant. In this case, three factors such as f, K, ρ^* are very important physical factors and then the following wave height spectrum is considered:

$$H(f) = f_3(f, \rho^*, K),$$
$$= G_3 K^{1/3} \rho^{*1/3} f^{-2/3},$$
$$\propto K^{1/3} \rho^{*1/3} f^{-2/3}, \quad \text{for } f_c < f < f_k \quad , \qquad (10)$$

where, G_3 is a non-dimensional coefficient.

Lastly, treat the very high frequency region ($f>f_k$) in which viscosity of water is only predominant. In this case, we can select only three factors such as f, ρ^* and μ^* as predominant physical factors. Therefore, the wave height spectrum given by Eq.(11) is considered,

$$H(f) = f_4(f, \varsigma^*, \mu^*),$$
$$= G_4 \cdot \mu^{*1/2} \varsigma^{*-1/2} f^{-1/2},$$
$$\propto (\mu^*/\varsigma^*)^{1/2} \cdot f^{-1/2}, \quad \text{---------- (11)}$$
$$\text{for } f > f_k .$$

By summarising the above-mentioned wave height spectra given by Eqs.(4), (6),(10) and(11), a wave height spectrum inside the surf zone may be expressed as shown in Fig.-1. From Fig.-1, it is easily understood that "-1power law ", "- 2 power law " ," -2/3 power law " and " -1/2 power law " are established in turn as the frequency f increases in the wave height spectrum. The coefficients, $G_1 \sim G_4$ express the levels of wave height spectrum and their features must be examined by various kinds of experiment.

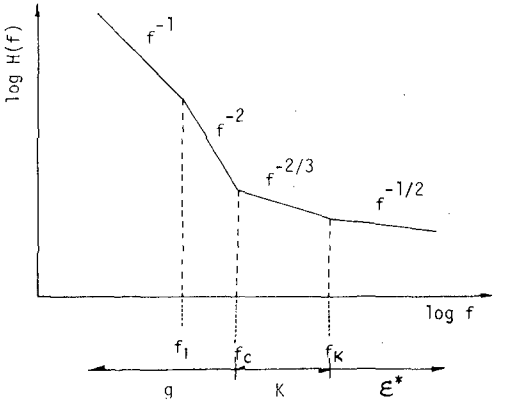

Fig.-1. Schematic view of wave height spectrum.

3 EXPERIMENTAL STUDY

1. Equipment and Procedures

Experiments were conducted to examine the characteristics of wave height spectra predicted by the dimensional analysis. In the experiments, an out-door wave tank in 0.65 m width, 0.95 m height,and 50 m length was used. At one end of the wave tank was installed a plunger-type wave generator and waves were able to be generated in different periods and amplitudes. At the other end of the tank, four kinds of beach slopes such as 1/15,1/25,1/40 and a composite slope consisting of an approach ramp with 1/12 slope leading up to a horizontal surface, were installed. Experimental conditions are shown in Table-1.

Wave profiles measured by a resistance-type wave gauge were recorded on magnetic tapes with 60 sec. periods and the data were sampled at each 1/50 sec. interval. Fourier analysis was carried out by FFT [4] method.

For each experimental run, by using a high speed cine-camera(100~200 frames/sec.), a breaking region was filmed through a grid on glass walls at the channel with the camera axis kept at a still water level. From these films, breaking points, breaking depths, domains of existence of horizontal rollers and the regions of air entrainment in breakers were decided.

2. Results and Discussion

Fig.-2 shows a change of wave height spectrum during wave propagation in the horizontal bed. In Fig.-2, the upper figure shows the characteristics of an incident wave, middle two figures are wave height spectra at a breaking point and at X/L=1.07 inside the surf zone, and the bottom figure shows the wave height spectrum of a reformed wave after passing through the surf zone. At the breaking point, the wave is composed of high frequency waves against the monocromatic frequency of an incident wave, and harmonic frequency component waves of an incident wave frequency are predominant. Inside the surf zone($0<X/L<1.30$), wave heights of the harmonic frequency waves grow larger than those of the incident wave and the reformed wave after passing through the surf zone. The reformed wave has no higher frequency component wave differing from waves inside the surf zone.

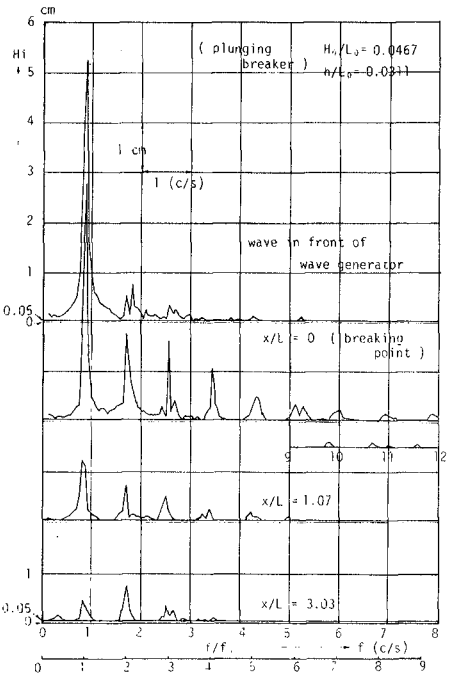

Fig.-2. Variation of wave height spectrum. (S = 0)

The fact that an incident periodic wave is transformed to a wave composed of its harmonic high frequency waves, shows the remarkable feature of breaking waves. Since wave breaking is non-linear phenomenon, waves in high harmonic frequency will grow due to non-linear terms of the wave motion. But , the effect of non-linear interaction among component waves may be small, because predominant periods of the component waves after breaking are, as mentioned above, harmonic periods of an incident wave period.

Now, consider the relation between a measured height $H_{ex.}$ and its Fourier component wave heights. The equivalent wave heights $H_{eq.}$ calculated by Eq.(11) obtained with the Parceval theorem have good agreement with the measured wave height $H_{ex.}$ as shown in Fig.-3. This shows that the measured wave can be treated as the sum of its Fourier component waves as follows:

$$H_{eq.} = \left(\sum_{j=1}^{\infty} H_j^2 \right)^{1/2}, \qquad \text{----------(11)}$$

where, $j=1 \sim \infty$ indicates Fourier component waves.

Fig.-4 and Fig.-5 show variation of wave height spectra plotted on log - log scale as waves propagate on a horizontal bed. Fig.-5 shows only predominant component waves. f_1 = 3.3 (c/s) and f_c = 13.3 (c/s) are obtained by Eqs.(2) and (5) for waves shown in Figs.-4 and -5, and the domain of air entrainment X_A/L is given to be $0 \leqq X_A/L \leqq 1.05$ for the wave shown in Fig.-4 and $0 \leqq X_A/L \leqq 1.30$ for the wave in Fig.-5 by the experiment.

Fig.-4 and Fig.-5 show that inside the surf zone with air entrainment, the slopes of wave height spectra are approximately proportional to " f^{-1} " for $f < f_1 = 3.3$(c/s) and " f^{-2} " for $f_1 = 3.3(c/s) < f < f_c = 13.3$(c/s). In cases of waves before breaking and waves after passing through the surf zone, however, the higher frequency component waves more than 5(c/s) can not be observed, and then, the slopes of wave height spectra are not proportional to " f^{-1} " and " f^{-2} " (see Fig.-4 (a),(g) and (h), and points X/L=2.99 and 3.04 in Fig.-5).

For the case of a spilling breaker , the slope of wave height spectrum at a breaking point is steeper than " f^{-2} " for $3.3(c/s) < f < 13.3(c/s)$ in Fig.-4(b) and, at the point X/L=0 in Fig.-5(a). This may be due to the reason that the turbulence of breaking is not saturated [5] all over the wave as shown in Fig.-6 and that the characteristics before breaking still remain. In the region such as X/L=0.322,0.523 and 0.775 in Fig.-4 where the turbulence of breaking is saturated, however, "-1 power law " and " -2 power law " are established as mentioned above.

Figs.-7 and -8 show variation of wave height spectra plotted on the log-log scale on a uniform slope of 1/40 and 1/25 respectively. Fig.-9 shows a change of wave height spectrum of predominant component waves piled up on the same graph, where h is a still water depth and h_b is a breaking depth. The characteristics of wave height spectra on uniform slopes are similar to those on the horizontal bed. As shown in Fig.-9, the slopes of wave height spectra are recognized to be nearly proportional to " f^{-2} " for the range of $f_1 < f < f_c$ independent of wave steepness,Ho/Lo, and beach slope,S. On the other hand, the slopes of wave height spectra for $f < f_1$ is roughly proportional to " f^{-1} ".

In sloping beaches, the values of wave height spectra decrease as waves propagate into shallower water depth as shown in Fig.-10, and inside the surf zone, the pattern of wave height spectrum such that a spectral slope is proportional to " f^{-1} " for $f < f_1$, and " f^{-2} " for $f_1 < f < f_c$, is still maintained. In Fig.-10, the point of $h/h_b = 0.19$ is outside the surf zone.

Summarizing the above-mentioned experimental results, it can be concluded that the wave height spectrum H(f) has the form of which slope is proportional to " f^{-1} " for $f < f_1 (= \sqrt{g/4\pi h})$ and to " f^{-2} " for $f_1 < f < f_c (= 1/2\pi\sqrt{S^* g/K})$ as critical wave height spectrum inside the surf zone where the turbulence of breaking is saturated all over the wave.

On the other hand, since values of wave spectra are very small at the present experiment for $f_c < f < f_k$ in which the surface tension is a restoring force, the characteristics may not be discussed sufficiently. But, in many experimental cases, it is recognized that the slope of wave height spectrum is approximately proportional to " $f^{-2/3}$ " as shown in Fig.-11. Therefore, it may not be said too much that " $f^{-2/3}$ " can be established.

For the frequency range of $f > f_k$ in which water viscosity is predominant, the authors can not discuss about " $f^{-1/2}$ " , because wave profiles were measured by using a low pass filter of which sheltering frequency is more than 25(c/s), and values of spectra are considerably small. In future, the authors will carry out large scale experiments and discuss in tetail.

Finally, variation of wave height of component waves will be discussed. The pattern of wave height decay of component waves is different between a spilling breaker and a plunging breaker.

As shown in Fig.-12(a), in case of the spilling breaker, high frequency wave heights grow larger once soon after breaking. On the other hand, in case of the plunging breaker, wave heights of high frequency waves decay uniformly after breaking as shown in Fig.-12(b). This difference may be due to the reason that the spilling breaker is not saturated by the turbulence of breaking at a breaking point, differing from the case of the plunging breaker.

The degree of wave height attenuation of component waves is generally larger as the frequency is higher, as shown in Fig.-12,where fo is the monocromatic frequency of an incident wave and f is the frequency of component waves. These mechanism may be due to the internal turbulent shear caused by breaking, and dissipating energy is proportional to υk^2(k=wave number, υ=kinematic viscosity) as predicted by the classical turbulence theory.

4.CONCLUSION

In this paper, the characteristics of wave height spectrum H(f) inside the surf zone of a monocromatic periodic wave are discussed.

Firstly, due to the dimensional analysis , it is predicted that there exist an critical wave height spectrum H(f) of which slopes are proportional to " f^{-1} " , "f^{-2} ", " $f^{-2/3}$ " and " $f^{-1/2}$ " in turn as the frequency f becomes larger.

Secondly, experiments were carried out to examine the results of the dimensional analysis. It is made clear that inside the surf zone, an incident monocromatic wave is transformed to a wave composed of high frequency component waves and that the subranges of "-1 power law ", " -2 power law " and " -2/3 power law" are established in the wave height spectrum as predicted by the dimensional analysis.

REFERENCES

1) Sawaragi,T and K. Iwata : On wave deformation after breaking. Proc. of 14th Conf. on Coastal Eng.,Copenhagen, Denmark, June 1974,pp.481 - 499.

2) Wiegel,R.L. : Oceanographical Engineering, Prentice-Hall, INC.,1964,pp.59 - 60.

3) Michell,A.G.M. : The heighest wave in water,Phil. Mag. Vol. 36(5),1893,pp. 430 - 437.

4) Cooley,J.W. and J.W.Tuckey : An algorithm for the machine calculation of complex Fourier series, Math.,Compt.,1965,pp.297 - 301.

5) Méhauté,B.L. : On non-saturated breakers and the wave run-up, Proc. of 8th Conf. on Coastal Eng., Mexico City, Mexico, 1963,pp.77 - 92 .

Notations	Values
S	0, 1/15, 1/25, 1/40
Ho/Lo	0.0031 - 0.1032

Table - 1. Experimental conditions.

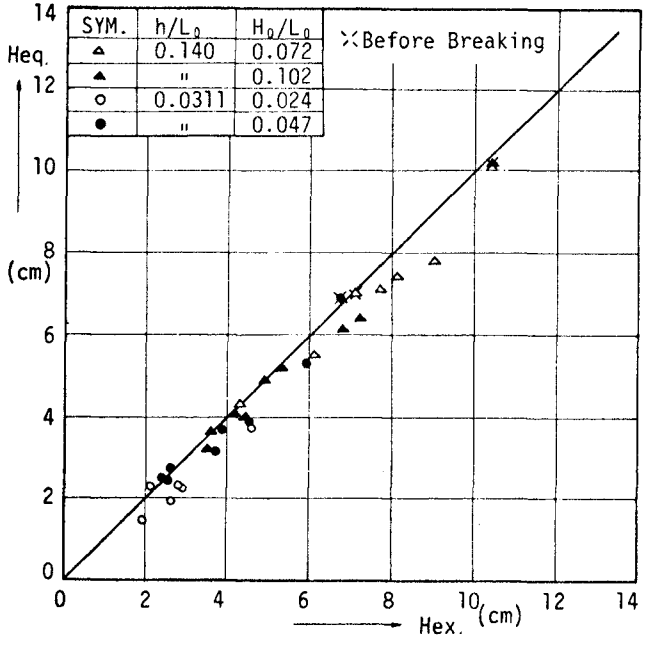

Fig. - 3. Relation between $H_{eq.}$ and $H_{ex.}$.

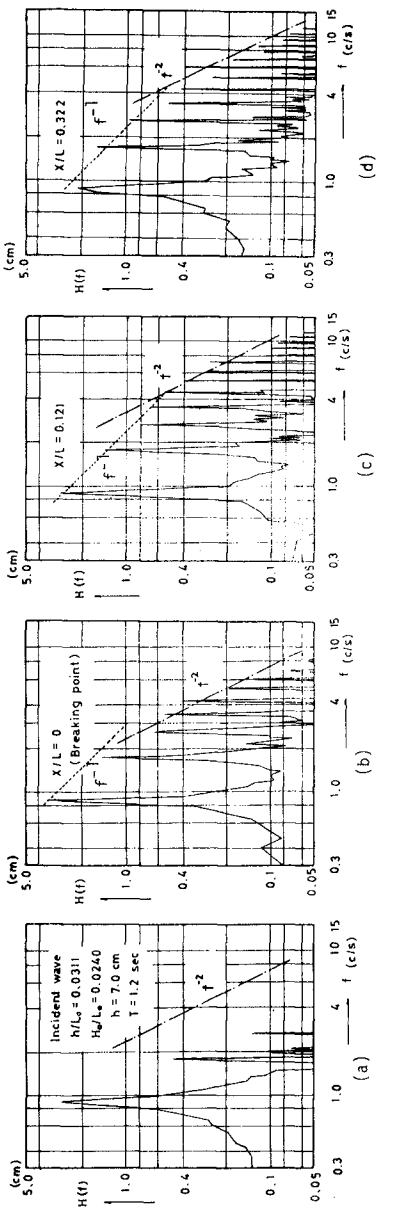

Fig. - 4. Variation of wave height spectrum. (S = 0)

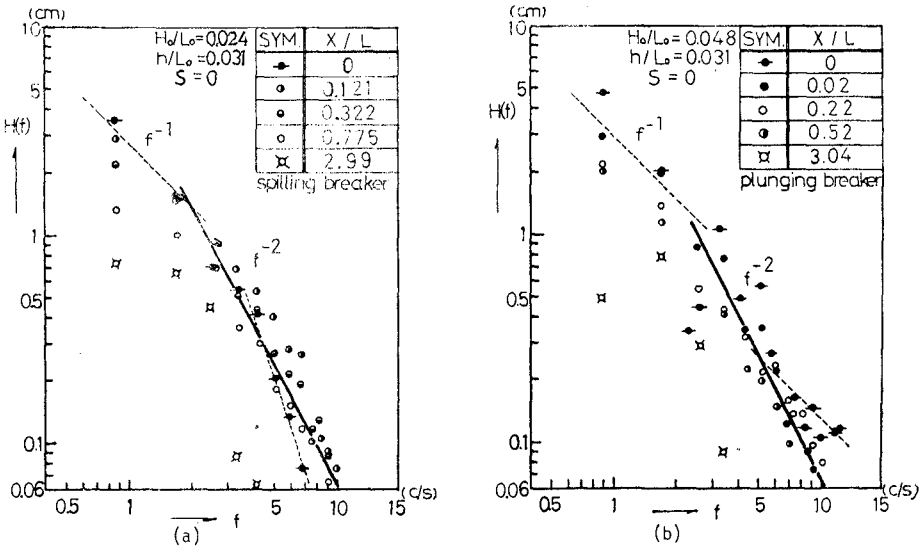

Fig. - 5. Variation of wave height spectrum. (S=0)
(Predominant components)

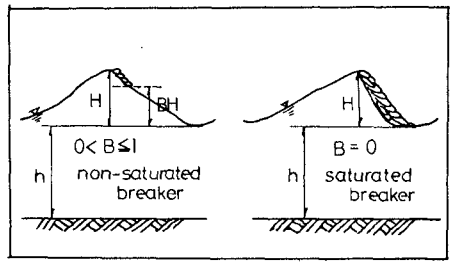

Fig. - 6. Schematic view of non-saturated breaker and saturated breaker.
(from Méhauté 5))

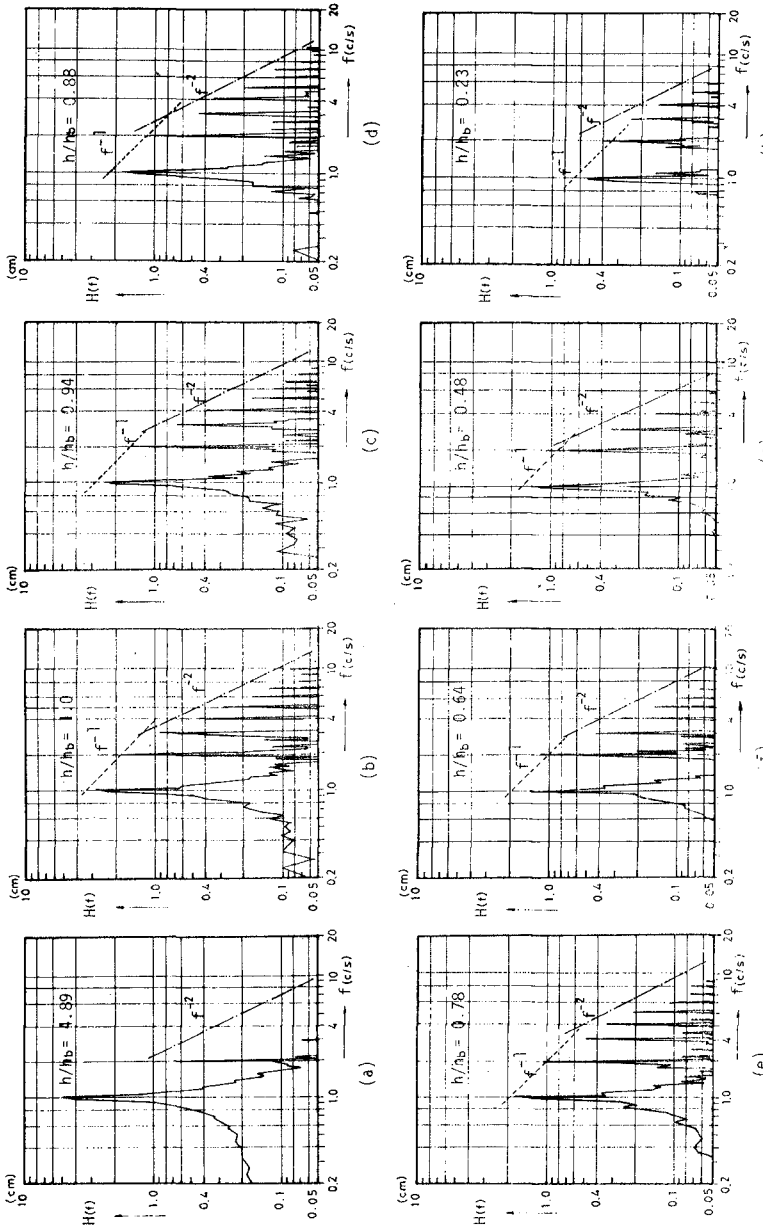

Fig. - 7 . Variation of wave height spectrum. (Ho/Lo=0.049, T=1.0 sec., S=1/40)

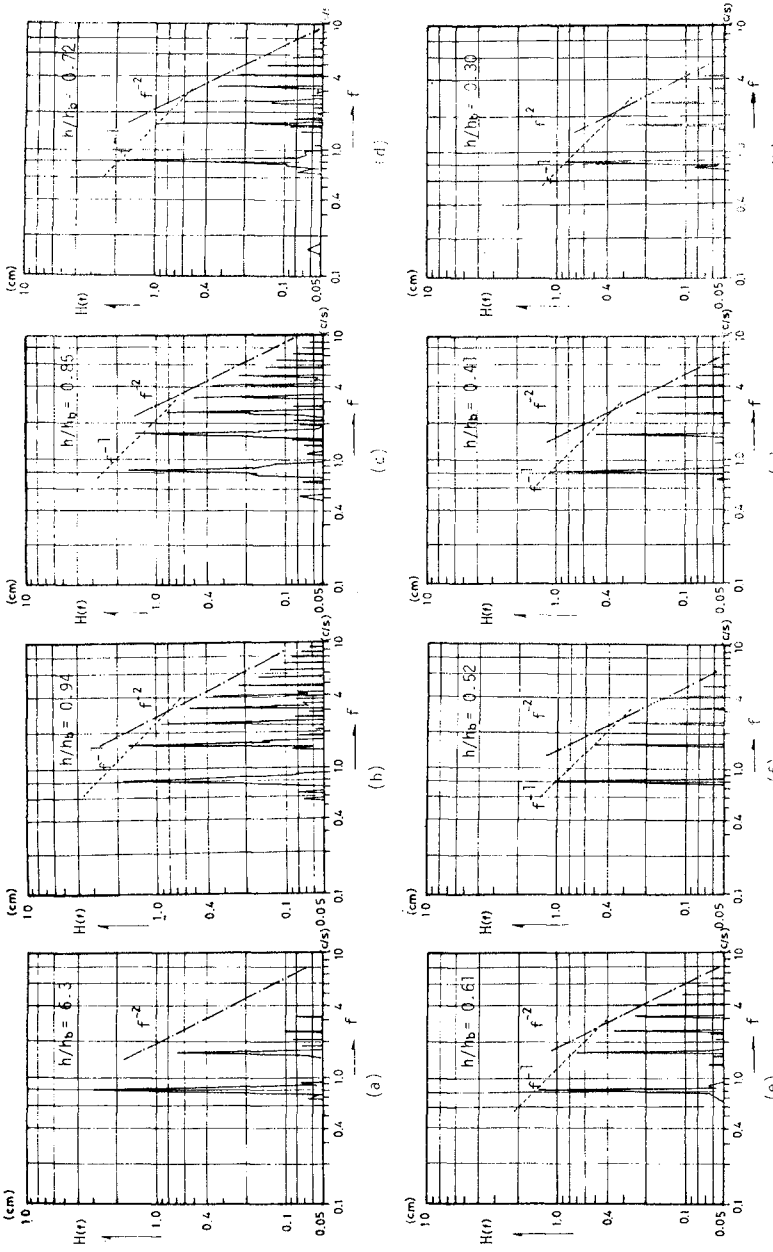

Fig. - 8 . Variation of wave height spectrum. (Ho/Lo=0.015, T=1.22 sec., S=1/25)

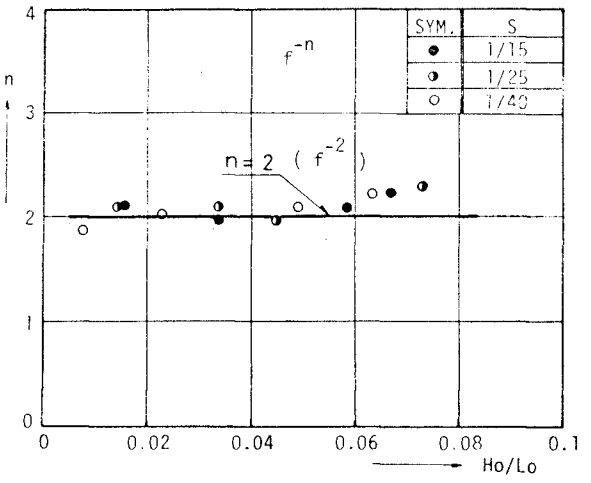

Fig. - 9. " -2 power law " .

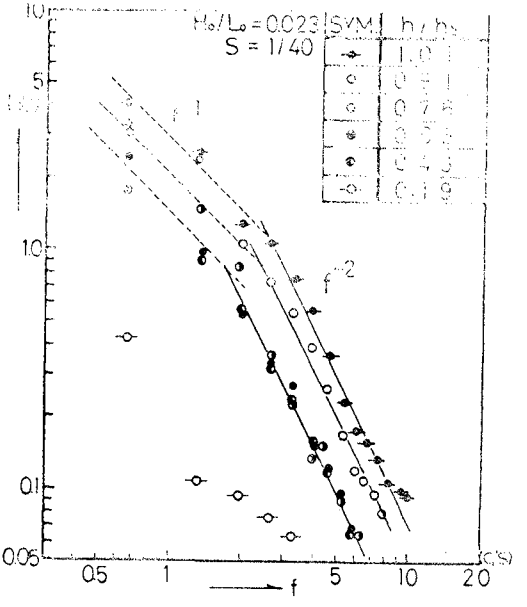

Fig. -10. Variation of wave height spectrum (S=1/40)
(Predominant components)

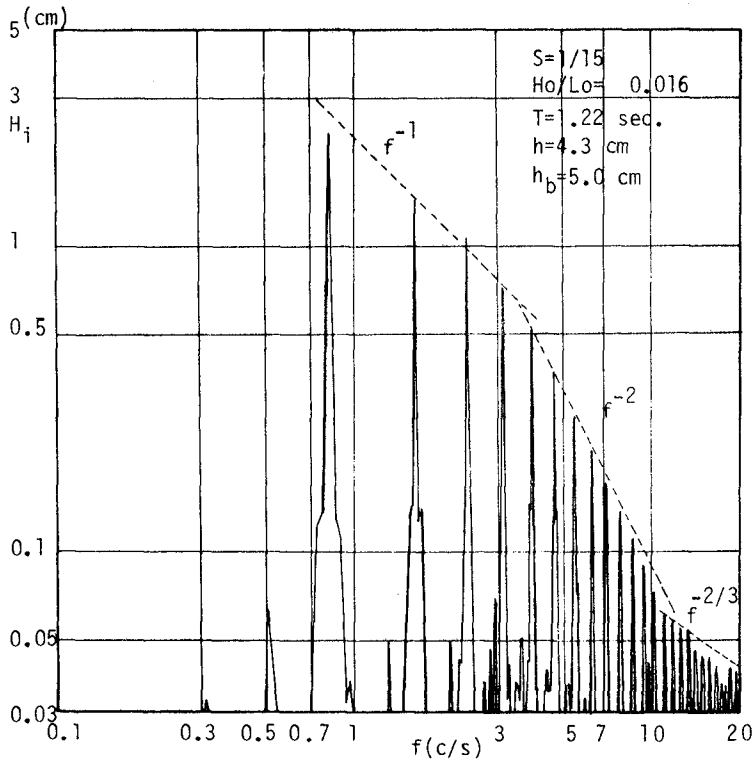

Fig. - 11. Wave height spectrum.

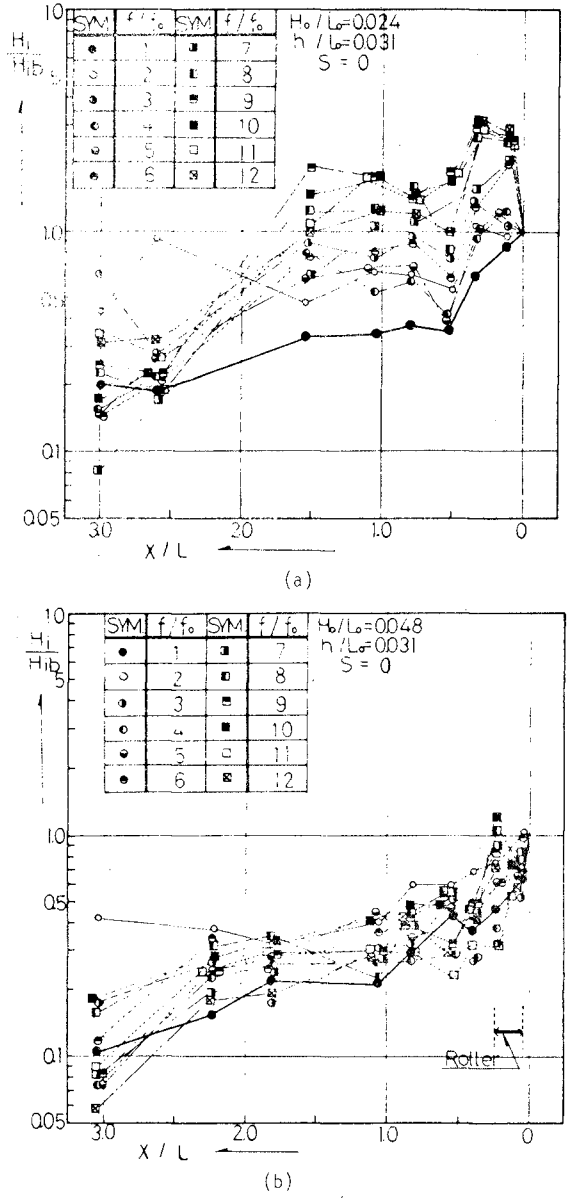

Fig.-12 . Attenuation of predominant component waves. (S = 0)
(H_i = wave height of component wave, H_{ib} =wave height of component wave at breaking point)